International Congress on Environmental Modelling and Software

8th International Congress on Environmental Modelling and Software - Toulouse, France - July 2016

Jul 12th, 4:30 PM - 4:50 PM

A numerical study of the lateral hyporheic flow about a channels confluence

C. Gualtieri
University of Naples Federico II, carlo.gualtieri@unina.it

International Environmental Modelling and Software Society (iEMSs)
8th International Congress on Environmental Modelling and Software
Toulouse, France, Sabine Sauvage, José-Miguel Sánchez-Pérez, Andrea Rizzoli (Eds.)
http://www.iemss.org/society/index.php/iemss-2016-proceedings

A numerical study of the lateral hyporheic flow about a channels confluence

C. Gualtieri

Department of Civil, Architectural and Environmental Engineering, University of Naples Federico II, Via Claudio 21, 80125 Naples, Italy; carlo.gualtieri@unina.it

Abstract: Stream and pore waters continuously interact and mix within streambeds due to spatial and temporal variations in channel characteristics. This mixing is termed as hyporheic exchange and the zone where groundwater and stream water are mixing is called hyporheic zone, which can greatly affect water quality is both surface and subsurface water systems. Typical examples of hyporheic fluxes are those under bedforms, intra-meander or across point bar deposits, while the lateral and vertical hyporheic exchanges about a riverine confluence was almost never investigated.
The paper presents some results of a numerical study carried out to investigate the basic features of the lateral hyporheic exchanges about the confluence of two channels. A 2D triangular geometry was used. Laminar flow in the channels and Darcian flow in the porous medium between them were considered. The simulations highlighted the role of the confluence planform and velocity ratio between the channels in controlling both the direction and the magnitude of the lateral hyporheic exchange.

***Keywords**:* Environmental hydraulics, CFD, river confluences, hyporheic flows

1 INTRODUCTION

Despite the traditional separation between the studies of surface water and groundwater flows, since some decades it has been recognized that rivers and aquifers are strongly connected and their interaction gives rise to a continuous exchange of water and solutes, which exerts a significant influence on the water quality. This analysis lead to identify a zone, termed *hyporheic zone*, where groundwater and stream water are mixing (Cushman-Roisin et al., 2012; Tonina, 2012). The hyporheic zone has hydrodynamical, physiochemical and biotic characteristics different from both the river and the subsurface environments and controls the distribution of solutes, colloids, dissolved gases and biogeochemical reactions from ripple to global scales (Huettel et al., 2003; Nishihara and Ackerman, 2012), and thus affects the distribution of benthic flora and fauna in lakes, oceans, bays and estuaries, as well as hyporheic and riparian organisms in rivers (Findlay, 1995). The effects of the hyporheic exchange processes on both the river and the subterranean environments are twofold. First, the hyporheic zone acts as a storage zone or a dead zone, which temporarily traps stream-transported solutes and then releases them after some time. Due to the low filtration velocities in the subsurface, the residence time of solutes in the hyporheic zone is usually much longer than the travel time in the main stream. This difference between the characteristic timescales of in-stream and hyporheic flow determines long tails in the time-concentration curves (Tonina, 2012). Second, the metabolic activity of the hyporheic microorganisms significantly alters the in-stream concentration of chemicals, both at the reach scale (Findlay et al., 1993) and at the basin scale (Harvey and Fuller, 1998). The surface of the hyporheic sediments is covered by biofilms of aerobic microorganisms, that use the dissolved oxygen from the surface water to oxidize nitrogen and phosphorus for their metabolism (Hancock et al., 2005). The hyporheic exchange is also important for riparian vegetation, as the oxygen flux from the stream regulates the redox conditions in the aquifer and therefore the dynamics of nutrients and trace metals (Brunke and Gonser, 1997). Typical examples of hyporheic fluxes are those under bedforms, intra-meander or across point bar deposits, which have received a significant attention in the recent literature (Bayani-Cardenas, 2008).
River confluences are an integral and relevant feature linking together the individual tributaries within river networks. The fluid dynamics about confluences have a highly complex flow structure with

several common types of flow features observed. It is generally acknowledged that the hydrodynamics and morphodynamics (i.e. patterns of erosion and deposition) within the confluence hydrodynamic zone (CHZ) are influenced by (1) the planform of the confluence; junction angle of confluence, (2) momentum flux ratio of merging streams (M_R) and (3) the level of concordance between channel beds at the confluence entrance (Best, 1987). Further any differences in the water characteristics (e.g. temperature, conductivity, suspended sediment concentration) between the incoming tributary flows and subsequent possible stratification may also impact on the local processes about the confluence (Trevethan et al., 2015; Gualtieri et al., 2015). Despite confluences are a common feature of riverine systems, there is a lack of knowledge about the lateral and vertical hyporheic exchanges at a fluvial confluence. Lambs (2004) studied the confluences between Garonne and Ariege rivers in the south-west of France and between Ganges and Yamuna rivers in the north of India. In the first case, localised groundwater outputs were detected 200 m before the confluence, while in the second a strong stream of groundwater output was measured at the point of confluence.
The paper presents some results of a numerical study carried out to investigate the basic features of the lateral hyporheic exchanges about the confluence of two channels. Two 2D triangular geometries with a different junction angle were used. Laminar flow in the channels and Darcian flow in the porous medium between them were considered. The simulations highlighted the role of the velocity ratio and the junction angle between the channels in controlling both the direction and the magnitude of the lateral hyporheic exchange as well as the flow about the confluence.

2 NUMERICAL SIMULATIONS

The analysis of the flow field in a free fluid-porous medium domain was carried out using numerical simulations. Free-fluid flow was simulated by using the well-known mass conservation and momentum balance equations. For a planar, steady-state, incompressible and laminar flow, they are:

$$\frac{\partial u}{\partial x}+\frac{\partial v}{\partial y}=0 \qquad 1)$$

$$\rho\left(u\frac{\partial u}{\partial x}+v\frac{\partial u}{\partial y}\right)=-\frac{\partial p}{\partial x}+\mu\nabla^2 u+F_x$$
$$\rho\left(u\frac{\partial v}{\partial x}+v\frac{\partial v}{\partial y}\right)=-\frac{\partial p}{\partial y}+\mu\nabla^2 v+F_y \qquad (2)$$

where in the Navier-Stokes equations, ρ is fluid density, μ is the dynamic viscosity, p is fluid pressure, F_x and F_y are force terms accounting for gravity or other body forces, and u, v are velocity components in the x and y directions, respectively.
In the porous medium, the governing equations are again continuity and momentum balance equations. For a planar, steady-state and incompressible flow, continuity equation is Eq. (1), while momentum balance equations in a porous medium are the empirical Darcy's law, which states that the volume averaged velocity field is determined by the pressure gradient, the fluid viscosity and the structure of the porous medium

$$\frac{\mu}{k}u=-\frac{\partial p}{\partial x}+F_x$$
$$\frac{\mu}{k}v=-\frac{\partial p}{\partial y}+F_y \qquad (3)$$

where k is porous medium permeability [L^2], which is a scalar for an isotropic porous medium.
These equations were solved using the Multiphysics™ modeling package, which is a commercial multiphysics modeling environment (Multiphysics, 2015).
Flows besides or over a porous medium are characterized by a hybrid free fluid-porous medium domain that flows both out and through the porous medium. The internal flow field of the porous medium remains coupled with the overlying fluid. The complex interaction between the overlying fluid and the internal fluid means the no-slip surface boundary condition is no longer applicable (James and Davis, 2001; Gualtieri, 2010). Thus, the fluid/porous interface problem, the flow interaction above and inside the porous medium, and the transfer mechanisms across the interface, deserve a careful

selection of the boundary conditions. In this study a two-ways coupling was implemented. ThisMultiphysics first solved Eqs. (1) and (2) for the pressure *p* and the velocity vector components *u* and *v* within the free fluid domain. Then, the calculated pressure distribution along the channel walls was assigned as a Dirichlet boundary condition for the groundwater flow equations and the flow field in the porous medium was solved. Finally, the darcian pressure distribution along the channel-porous medium interface was assigned as a Dirichlet boundary condition for the free flow domain and here the flow field was again calculated. Past studies have usually applied a sequential coupling where the last step was not included (Bayani-Cardenas and Wilson, 2007; Gualtieri, 2012, 2014).

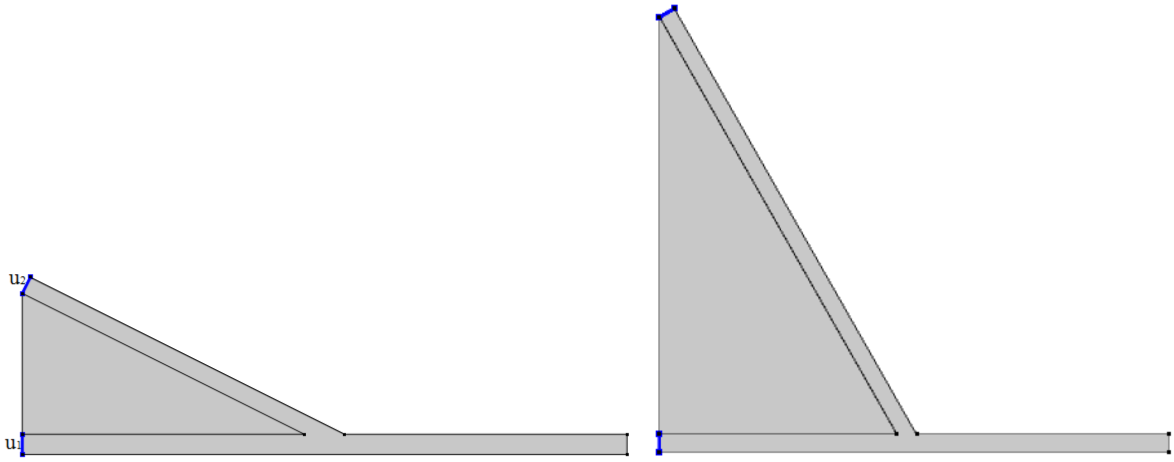

Figure 1. The investigated geometries.

Multiphysics 4.4™ was applied to the two 2D triangular geometries, which represent a confluence of two channels which includes a porous medium (Fig.1). Geometry A and Geometry B have a junction angle of 30° and 60°, respectively. In each geometry, two inflows are entering in each channel. The channels were 1.0 m wide. Channel 1, i.e. the main stream, was 30 m long, while the channel 2, i e. the tributary channel, length depended on the junction angle. The confluence was located at 14 m downstream of channel 1 inlet. Flow conditions were characterized using the ratio between the flow velocities defined as:

$$U_R = \frac{u_1}{u_2} \tag{4}$$

This parameter can approximate the momentum flux ratio because the inflows have the same density and width. Six values of U_R were considered. They are listed in Table 1

Geometry	Run	U_R	Remarks
A	A1	0.10	
A	A2	0.25	
A	A3	0.50	
A	A4	1.00	
A	A5	2.00	
A	A6	5.00	
B	B1	0.10	
B	B2	0.25	
B	B3	0.50	
B	B4	1.00	
B	B5	2.00	
B	B6	5.00	

Table 1. Runs performed – Hydrodynamics conditions.

For the simulations water at 20 °C with density ρ=998.16 Kg/m³ and dynamic viscosity μ=1.00×10^{-3} was selected for the fluid properties. The intrinsic permeability of the porous medium *K* was set to 1×10^{-10} m², which corresponds to well-sorted coarse sand. Boundary conditions were assigned in both the sub-domains:

- at the inlets, a *normal flow* type condition was assigned;
- at the walls, a *no-slip* condition was assigned;
- at the outlet, a *zero pressure* type condition was assigned;
- the left boundary of the porous domain was considered as *impermeable*.

Different mesh characteristics were tested. This is a very important point in any CFD simulation (Blocken and Gualtieri, 2012). For both Geometry A and B, the finer values of the element size were assigned at the interface between the free flow domain and the porous medium to better capture the hyphoreic exchange (Fig.2). The mesh for geometry A and B has 25239 and 12308 elements, respectively, with an average *element quality* of 0.897 and 0.905, respectively. The *element quality* measure is related to its aspect ratio, which means that anisotropic elements can get a low quality measure even though the element shape is reasonable (Multiphysics, 2013). It is a scalar from 0 to 1. Mesh quality visualization demonstrated a quite uniform quality of the elements of the mesh.

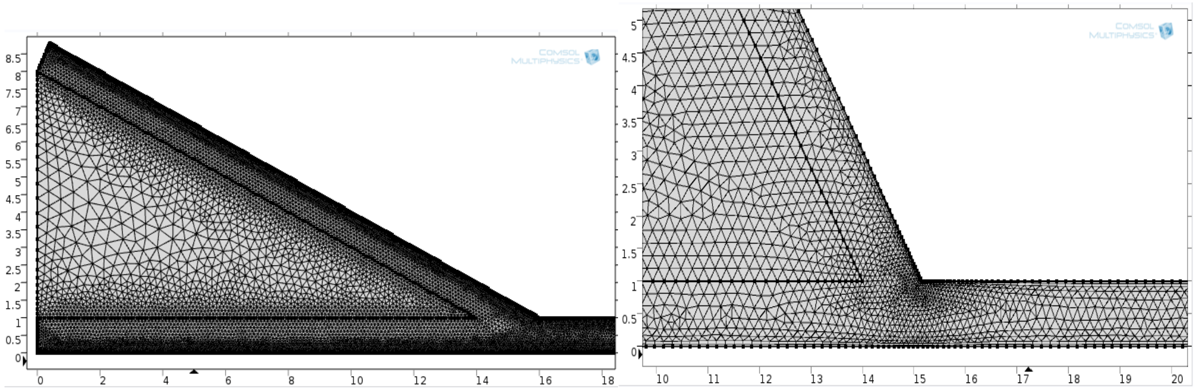

Figure 2. Mesh for Geometry A (left) and Geometry B (right)

About the solver settings, stationary segregated solver with non-linear system solver was used, where the relative tolerance and the maximum number of segregated iterations were set to $1.0 \cdot 10^{-3}$ and 100, respectively. The segregated solver allows to split the solution steps into sub-steps. These are defined by grouping solution components together. This procedure can save both memory and assembly time. Two groups were considered, namely the velocity components and pressure in the channels and in the porous medium.

3 NUMERICAL RESULTS AND DISCUSSION

Numerical simulations provided velocity field and pressure values throughout the flow domains. The analysis of results was first focused to characterize the flow field in the area of the confluence. Fig.3 shows the flow field about the confluence for the lowest velocity ratio in both the geometries, i.e. A1 and B1 runs. As expected, flow deflection and separation is larger with the larger angle of junction.

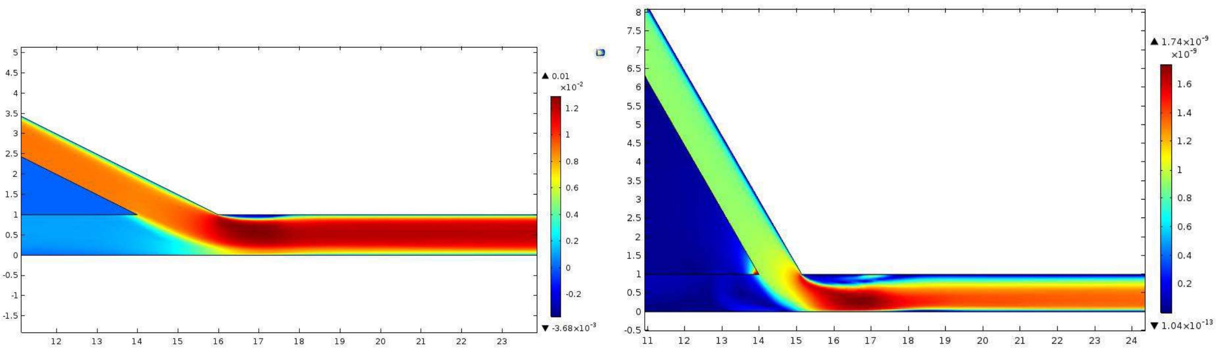

Figure 3. Flow field in the area of the confluence for A1 (left) and B1 (right)

A comparison of the flow field about the confluence in the Geometry B for Runs B2 and B6 shows that all the key features of a confluence hydrodynamics can be observed: stagnation zone (3); region of deflection (4); downstream separation zone (5) and region of maximum velocity (6), while (1) and (2) are the incoming flows (Fig.4). However, these features had different extension and strength. As expected, the size of the downstream separation region was larger in B2, where the tributary had the larger inflow velocity. On the opposite, the strength of the maximum velocity was larger in B6, where the main channel had the larger inflow velocity.

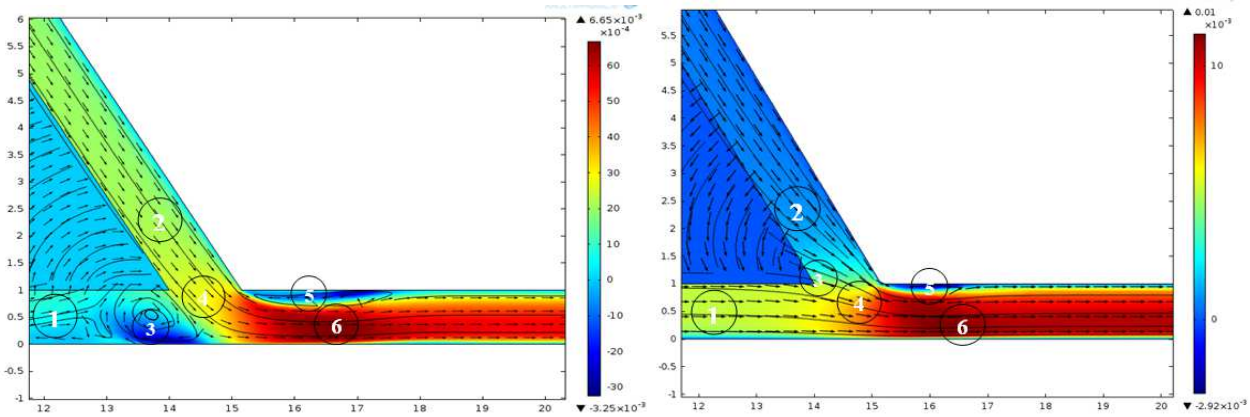

Figure 4. Flow about the confluence for Run1 B2 (left) and B6 (right)

Moreover, a closer inspection of the flow field about the confluence in the Geometry B for the Runs with the lowest U_R, i.e. B1 and B2, revealed how the hydrodynamic features about a confluence interacted with the hyporheic flow in the porous medium upstream of the confluence (Fig.5). In the stagnation region of the main channel a recirculation flow was observed, which created an hyporheic flow from this channel into the porous medium just in the junction corner.

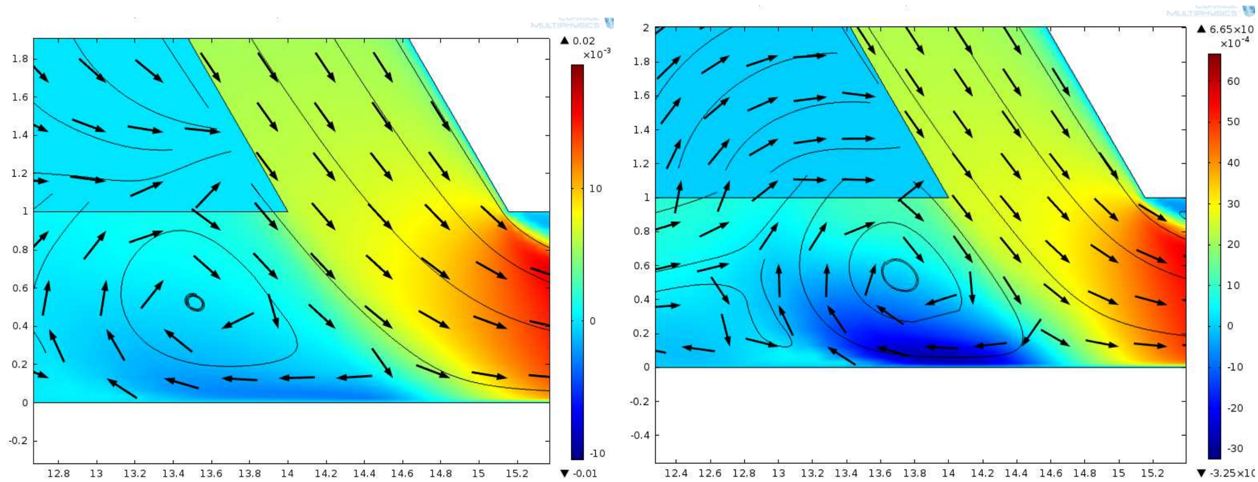

Figure 5. Enlarged picture of the flow about the confluence for Run B1 (left) and B2 (right)

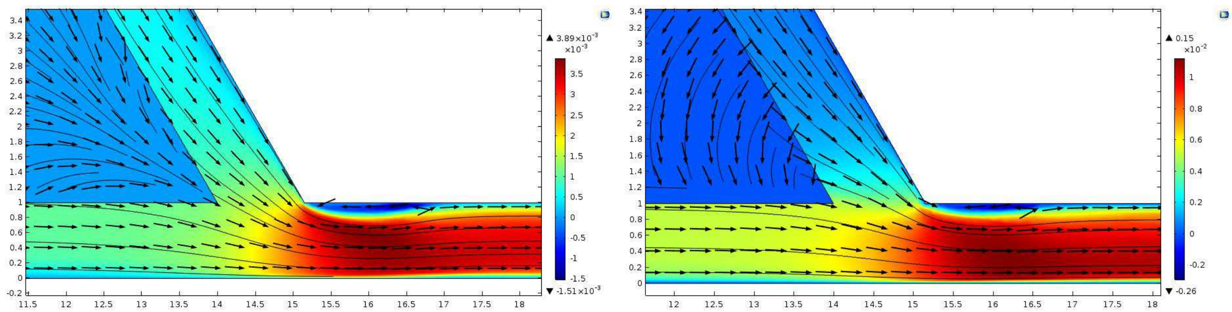

Figure 6. Flow about the confluence for Run B4 (left) and B6 (right)

At larger U_R, for Runs B4 and B6, as the flow in the main channel tended to be predominant, the size of the separation region was lower and the flow recovery was faster (Fig.6). Moreover, for Run B4, where U_R=1, the hyporheic flow in the junction corner arrived from both channels (Fig.6, left), while at the largest U_R, for Run B6, the hyporheic flow was from the tributary to the porous medium in the junction corner and even upstream.

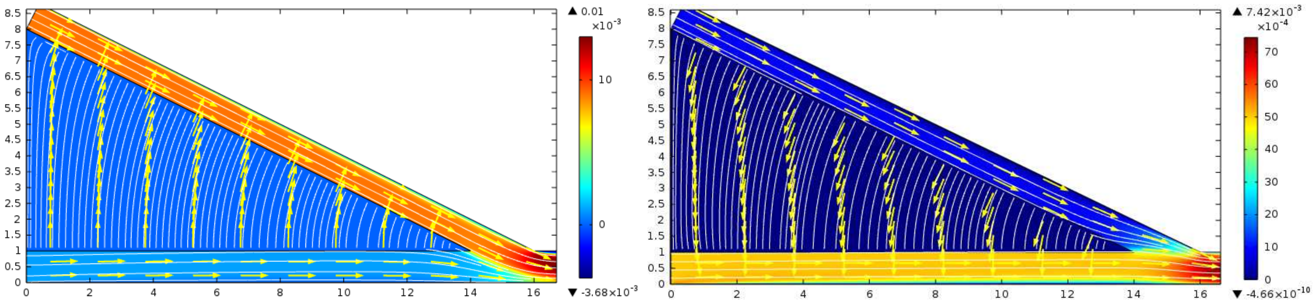

Figure 7. Flow field in the Geometry A for Run A1 (left) and A6 (right)

Fig.7 shows the flow field in the Geometry A at the lowest (A1) and at the highest (A6) velocity ratio. Following the pressure gradient between the internal walls of the channels, the hyporheic flow was from the channel with the lower velocity (blue colour) to the channel with the larger velocity (orange or red colour). The streamlines in the porous medium were almost vertical.
Even in Geometry B, the hyporheic flow was from the channel with the lower velocity to the that with the larger velocity (Fig.8) due to the pressure gradient existing in the porous medium (Fig.9). In Geometry B, the streamlines in the porous medium had different curvature depending from the location in the main channel (Fig.9, left).

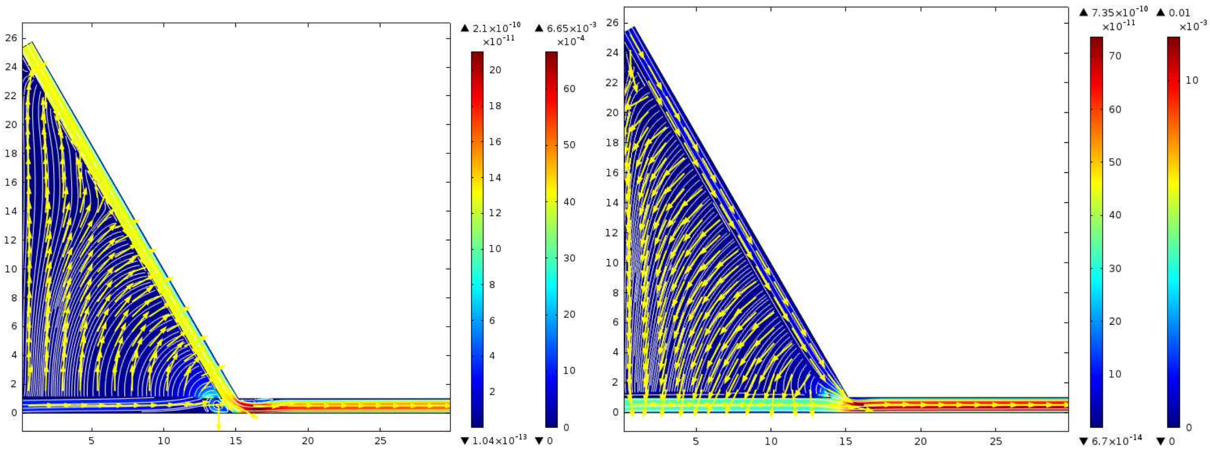

Figure 8. Flow field in the Geometry B for Run B2 (left) and B6 (right)

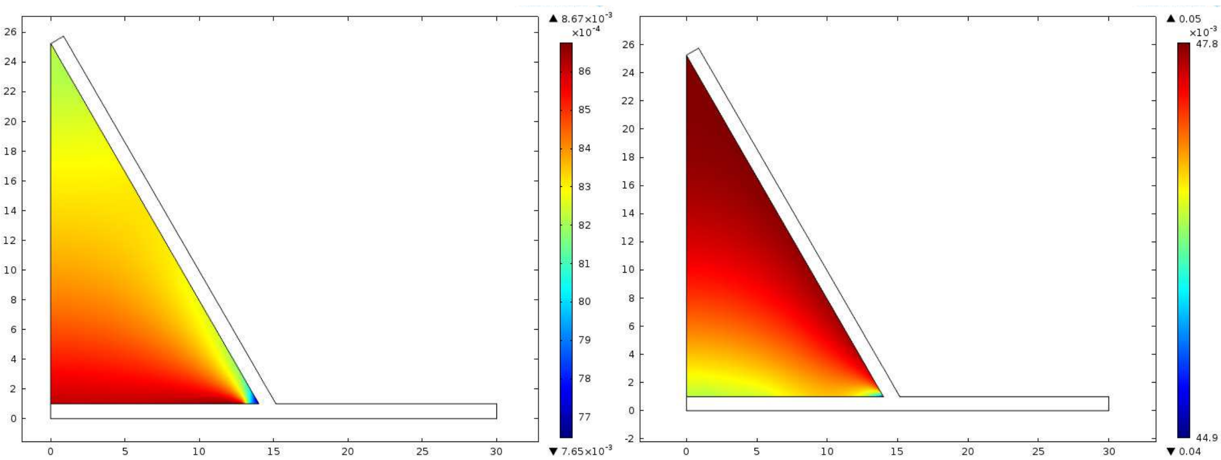

Figure 9. Pressure field in the porous medium in the Geometry B for Run B2 (left) and B6 (right)

4 CONCLUSIONS

The paper presented the results of a numerical study to investigate the basic features of the lateral hyporheic exchange about the confluence of two channels. Two triangular geometries with a different value of the junction angle were considered. For each geometry, six simulations in laminar flow conditions were performed with a different value of the velocity ratio.

The analysis of the numerical results highlighted the role of the junction angle and the velocity ratio in controlling the flow field in the channels and in the porous medium. First, the hydrodynamic features commonly observed about a confluence, such stagnation, deflection, separation and maximum velocity regions, were observed. Second, their extension and strength were related both to the junction angle and the velocity ratio. Third, in the geometry with the larger junction angle, these hydrodynamic features interacted with the hyporheic flow in the junction corner of the porous medium. Fourth, following the pressure gradient between the internal walls of the channels, the hyporheic flow was from the channel with the lower velocity to that with the larger velocity. Also, the curvature of the streamlines of the hyporheic flow were related to the characteristic of the geometry.

Overall, it can be concluded that about a channel confluence, significant hyporheic flows could be expected, whose characteristics are related to both the confluence planform and the velocity/momentum flux ratio between the confluents.

ACKNOWLEDGMENTS

The author acknowledges the preliminary work carried out by his former students B.Mancino, F.Miccio, L.Mollettieri, M.Onorato, G.Sorrentino e E.Toscano.

REFERENCES

Bayani-Cardenas, M., 2008. The effect of river bend morphology on flow and timescales of surface water–groundwater exchange across pointbars, Journal of Hydrology, 362, 134–141

Bayani-Cardenas, M. and Wilson, J.L., 2007. Hydrodynamics of coupled flow above and below a sediment–water interface with triangular bedforms, Advances in Water Resources, 30(1), 301–313

Best, J. (1987). *Flow* dynamics at river channel confluences: implications for sediment transport and bed morphology*. Recent Developments in Fluvial Sedimentology*, (Eds. Ethridge, F., Flores, M. and Harvey, M.,), Spec. Publ. 39, Society of Economic Paleontologists and Mineralogists, 27-35.

Blocken, B., Gualtieri, C. (2012). Ten iterative steps for model development and evaluation applied to Computational Fluid Dynamics for Environmental Fluid Mechanics. Environmental Modelling & Software, vol.33, n.7, July 2012, pp.1−22, DOI 10.1016/j.envsoft.2012.02.001

Brunke, M. and Gonser, T., 1997. The ecological significance of exchange processes between rivers and groundwater, Freshwater Biol., 37, 1–33

Cushman-Roisin, B., Gualtieri, C., Mihailović, D.T., 2012. Environmental Fluid Mechanics: Current issues and future outlook. In: Gualtieri, C., Mihailović, D.T. (Eds), Fluid Mechanics of Environmental Interfaces, 2nd ed., CRC Press/Balkema, Leiden, Holland, 3-17.

Findlay, S., Strayer, D., Goumbala, C., and Gould, K., 1993. Metabolism of streamwater dissolved organic carbon in the shallow hyporheic zone. Limnol.Oceanogr., 38 (7), 1493–1499

Findlay, S., Importance of surface-subsurface exchange in stream ecosystems: The hyporheic zone, 1995. Limnol. Oceanogr., 40(l), 159–164

Gualtieri, C. (2010). Numerical simulation of transition layer at a fluid-porous interface. In D.A. Swayne, W. Yang, A.A. Voinov, A. Rizzoli, T. Filatova (Eds.): Modelling for Environment's Sake. Proceedings of the iEMSs Fifth Biennial Meeting: International Congress on Environmental Modelling and Software (iEMSs 2010), Ottawa (Canada), July 5/8, 2010, Vol.I, pp.399−409

Gualtieri, C. (2012). Effect of permeability on hyporheic flows across a triangular dune. In D.T.Mihailović (Editor): Essays on Fundamental and Applied Environmental Topics, pp.355, Nova Science, New York, USA, pp.115–132 (ISBN 978−1−61942−522−4)

Gualtieri, C. (2014). Bedforms-induced hyporheic exchange: impact of the porous medium permeability. In D.P. Ames, N.W.T. Quinn, A.E. Rizzoli (Eds.): Bold Visions for Environmental Modelling. Proceedings of the iEMSs Seventh Biennial Meeting: International Congress on Environmental Modelling and Software (iEMSs 2014), S.Diego, USA, June 15/19, 2014

Gualtieri, C., Trevethan, M., Ianniruberto, M., Filizola, N., De Oliveira, M., Martinelli Santos, A. (2015). Hydrodynamics and mixing at the confluence of Rio Negro and Rio Solimões. Andean and Amazonian rivers: deciphering the global change from the hydroclimatic variability in the critical zone, 6th Observation Service HYBAM Scientific Meeting, Cusco (Perù), October 26/30, 2015

Hancock, P., Boulton, A., and Humphreys, W., 2005. Aquifers and hyporheic zones: Towards an ecological understanding of groundwater. Hydrogeol. J., 13, 98–111

Harvey, J.W. and Fuller, C.C., 1998. Effect of enhanced manganese oxidation in the hyporheic zone on basin-scale geochemical mass balance. Water Resour.Res., 34(4), 623–636

Huettel, M., Røy, H., Precht, E., and Ehrenhauss, S., 2003. Hydrodynamical impact on biogeochemical processes in aquatic sediments., *Hydrobiologia*, 494 (3), 231–236

James, D.F., and A.M., Davis, 2001. Flow at the interface of a model fibrous porous medium., *J. Fluid Mechanics*, 426, 47–72

Lambs, L., 2004. Interaction between groundwater and surface water at river banks and the confluence of rivers, Journal of Hydrology, 288, 312–326

Multiphysics 4.4, 2013. User's Guide, ComSol AB, Sweden

Nishihara, G.N., and J.D. Ackerman, 2012. Mass transport in aquatic environments. in*:* Gualtieri, C. and Mihailović, D.T., (Eds.), Fluid mechanics of environmental interfaces, Taylor & Francis Ltd, London, 423–451.

Tonina, D. 2012. Surface water and streambed sediment interaction: the hyporheic exchange. in*:* Gualtieri, C. and Mihailović, D.T., (Eds.), Fluid mechanics of environmental interfaces, Taylor & Francis Ltd, London, 255–294.

Trevethan, M., Martinelli, A., De Oliveira, M., Ianniruberto, M., Gualtieri, C. (2015). Fluid dynamics, sediment transport and mixing about the confluence of Negro and Solimões rivers, Manaus, Brazil. XXXVI IAHR Congress, Delft–The Hague, The Netherlands, June 28 / July 3, 2015